

An Asymmetry Descriptor for Melanoma Diagnosis

Zhao Liu¹

zhao.liu@uwe.ac.uk

Jiulai Sun¹

jiulai2.sun@uwe.ac.uk

Melvyn Smith¹

melvyn.smith@uwe.ac.uk

Robert Warr²

robert.warr@nbt.nhs.uk

Lyndon Smith¹

lyndon.smith@uwe.ac.uk

¹ Machine Vision Lab

University of the West of England

Bristol, UK

² Plastic Surgery

Frencahy Hospital,

NHS, UK

Abstract

This paper proposes a novel reflectional asymmetry descriptor to quantize the asymmetry appearance of melanocytic lesions. The new reflectional asymmetry descriptor based on global point signatures (GPS) of the pigmentation model enable to characterize the shape and pigmentation information simultaneously. The experiment results from 311 dermoscopy images shows that the proposed asymmetry descriptor has more discrimination power than descriptors without GPS, which gives 85.12% sensitivity and 76.38% specificity for melanoma diagnosis.

1 Motivation

Asymmetric appearance usually represents an abnormal reproduction of biological cells within body organs and tissues, with probability to become metastatic and aggressively spread thorough the body. Malignant melanoma, which accounts for 75% mortality caused by skin cancers [1], is one of these examples. Accordingly ABCD rules- standing for asymmetry (A), border irregularity (B), colour variegation (C) and diameter of the lesion (D)- have been developed for clinical diagnosis to identify melanoma. In particular, asymmetry characterizing the extrinsic contour or shape of the lesion has been transferred into automatic computed quantities. Stoecker et al. [2] computed the principal axes and determined the reflectional asymmetry of the lesion in terms of area differences across axis. Andreassi et al. [3] segmented a lesion across 360 axes and exploited the variance of area differences to generate a contour asymmetry measure. Stanganelli et al. [4] used the size function to quantify the shape and colour asymmetric appearance of the two-halves of the lesion. However, these asymmetry detection approaches share some similar shortcomings. Firstly, most of the existing asymmetry descriptors are shape dependent or sometimes colour dependent alone, while dermatologists comprehensively analyze both during clinical diagnosis. Secondly, recent approaches simply combined the shape and colour asymmetry descriptors. But separating shape and colour asymmetry detection might yield two different reflectional axes.

This paper proposed a new asymmetry descriptor able to simultaneously quantify the spatial and colour distributions of the cutaneous lesions. A pigmentation model is constructed by mapping colour information, like red, green or blue values in an RGB image, to the third axis of a Cartesian coordinate. Then the global point signatures (GPSs) of the pigmentation model are applied to measure the reflectional asymmetry of the lesion by minimizing the histogram difference of the GPSs. Compared with asymmetry descriptor without GPSs, the proposed asymmetry detector proved more efficient in describing the abnormality of the cutaneous skin lesions.

2 Methodology

2.1 Pigmentation Modelling

Several pre-processing steps are applied to remove the hairs on the skin [5], flatten the homogeneous regions meanwhile preserve the edges [6], and isolate the areas of pigmented skin lesions from the surrounding normal skin [7]. Then the pigmentation model is constructed by assigning colour values as Z axis, and spatial information of the isolated lesion as X and Y axes respectively. In order to make the spatial and pigmentation provide comparable contributions when building the asymmetry descriptor, the model is scaled down in a bound box as follow. First normalize the X_{lesion} so that its range is 1 (supposing X_{lesion} has larger range than Y_{lesion}). Then compress the Y_{lesion} to the range of r , where $r = Y_{lesion}/X_{lesion}$. Finally Z axis representing colour information is normalized to the range of [0 1] by dividing 255.

Figure.1 shows the pigmentation models calculated from an isolated malignant melanoma (MM) and a benign nevus (BN) images. The outer boundary of the shape stands for the spatial distribution of the lesion, and the pigmentation asymmetry can be reflected by the asymmetry of the pigmentation model along Z direction.

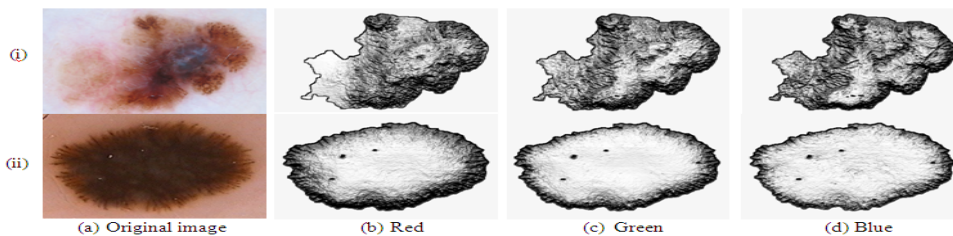


Figure 1: Pigmentation model from dermatoscopy images. (i) MM (ii) BN.

2.2 Computing the GPSs

The proposed asymmetry descriptor is based on GPSs, which are derived from Laplace Beltrami operator [8]. The Laplace Beltrami operator is defined as the divergence of the gradient on a surface function in Riemannian manifold and it can be approximated by the graph Laplacian matrix by heat kernel [9], where the eigenvectors of the Laplacian matrix embed the points on the manifold to low dimensional representations. GPSs are used because they integrate the shape and colour information on the pigmentation model simultaneously. Moreover, it has been proved that GPSs are robust to the metric deformations [10] which might be introduced by the camera positions or various lighting conditions during data acquisition.

Suppose a set of feature vectors $x_1, x_2, \dots, x_\omega \in M$ and M is a d -dimensional Riemannian manifold. An adjacency graph connecting edges between points can be constructed by computing the heat kernel W_{ij} as,

$$W_{ij} = \begin{cases} e^{-\frac{(x_i - x_j)^2}{4\sigma}} & \text{if } x_j \text{ is the } k \text{ nearest neighbor of } x_i \\ 0 & \text{otherwise} \end{cases} \quad (1)$$

where t is the standard deviation of neighbour points, and k is the number of nearest neighbours. Then the Laplace matrix L can be calculated as $L = D - W$, where D is a diagonal weight matrix with the entries $D_{ii} = -\sum_j W_{ij}$. Since the Laplace matrix is symmetric, negative and semi-defined, it has an eigen-decomposition with a set of eigenvectors ϕ_u and the corresponding eigenvalues λ_u as $L\phi_u = \lambda_u D\phi_u$ ($0 = \lambda_0 < \lambda_1 < \lambda_2 < \dots < \lambda_{\omega-1}$). The manifold M can then be embedded in the GPS spaces [8] as,

$$gps(p) = \left\{ \frac{\phi_1(p)}{\sqrt{\lambda_1}}, \frac{\phi_2(p)}{\sqrt{\lambda_2}}, \dots, \frac{\phi_u(p)}{\sqrt{\lambda_u}}, \dots \right\} \quad (2)$$

In our work, M is the pigmentation model in 3-dimensional space. The eigenvectors corresponding to the first few eigenvalues determine the optimal embeddings. In practice, the first eigenfunction with $\lambda_0 = 0$ is neglected because it generates a constant function. In addition, the eigenfunctions associated with repeated eigenvalues could introduce rotational symmetries that are not stable for small non-isometric perturbations [10]. Therefore we restrict our searching for reflectional asymmetry detection in the first 6 eigenfunctions with non-zero and non-repeated eigenvalues.

2.3 Reflectional Asymmetry Descriptor

Because the Laplace operator L uniquely determines the metric of the manifold, M is intrinsically symmetric if there is a self-mapping $T : M \rightarrow M$, making both ϕ_u and $\phi_u \circ T$ the eigenvectors of L . Suppose gps_u is the u^{th} ($1 < u < 6$) component in the GPSs with $p \in M$, and $T = \{t_1, t_2, \dots, t_6\}$ be the sign sequence. For a complete symmetric object, the GPSs with non-repeated eigenvalues only holds two possible mappings around the reflectional symmetry axis as $gps_u \circ T = gps_u$ and $gps_u \circ T = -gps_u$. As such, the selfmapping T can be determined by a sign sequence with entries of either positive (+1) or negative (-1). But because skin lesions are not the exact symmetric object, the complete symmetry measure $|gps(p) \circ T| = |gps(p)|$ will not fulfil. We thus generate a region-based descriptor in histogram to quantify the reflectional asymmetry distribution of the skin lesion in the GPSs.

The gravity centroid of a lesion is first defined, and the lesion is segmented into 180 segments around the polar coordinate across the centre. For each segment, we built the histogram with 100 bins, and the descriptor of each segment l in signature u is,

$$Des_{u,l}(T) = \frac{1}{N_l} \sum_{n=1}^{100} f(gps_{u,l}^n(T)) * v(gps_{u,l}^n(T)) \quad l = 1, 2, \dots, 180 \quad (3)$$

where f represents the frequency counts in each bin, v is the bin location of $gps_{u,l}(T)$ in histograms and N_l is the number of pixels in each segment.

For a single $gps_u(T)$, the $Des_u(T)$ value can be plotted in 1D space from 0 to π . As the principal axis must exist in these 180 segments, we assume one segment as the principal axis at each time, and translate part of the $Des(T)$ to ensure 90 elements on both sides along the axis. The values of histogram on the left and right sides are then compared by minimizing the Euclidean distance to find the optimal reflectional symmetry plane. Considering there are 6 GPSs, the asymmetry degree of a dermoscopy image can be quantified as,

$$Asy(T) = \min \left(\sum_{u=1}^6 \sum_{l=1}^{90} \|Des_{u,l}^L(T) - Des_{u,l}^R(T)\|_2^2 \right) \quad (4)$$

where $Des_{u,l}^L$ represents the left side and $Des_{u,l}^R$ stands for the right part of the histogram. Because the asymmetry descriptor is a function of the sign sequence T , the minimum asymmetry measure also indicates the potential optimal reflectional axis. So the process integrates the asymmetry measure and the reflectional axis searching simultaneously. Moreover, since GPSs integrate the shape and colour asymmetry detections simultaneously, it avoids

the problem of yielding two different symmetry planes when the symmetric appearance of shape and colour are analyzed separately.

Figure.2(i) show the images corresponding to the first 6 GPSs with optimal T computed from blue channel in RGB images of the MM and the BN in Figure.1. All the $gps(T)$ from the BN display approximate symmetric appearance in a given direction, whereas it is difficult to find an appropriate symmetry plane fit for all the $gps(T)$ of the MM. The first two $gps(T)$ are usually indicators for shape asymmetry quantization, while higher orders of $gps(T)$ reflect the pigmentation asymmetry inside the lesion. Figure.2(ii) plots the translated histograms with minimum asymmetry measure of the GPSs. The BN shows symmetric appearance on left-right side of the translated histograms, while the optimal translated histograms of the MM greatly fluctuate, which result in a large asymmetry measure for classification purpose.

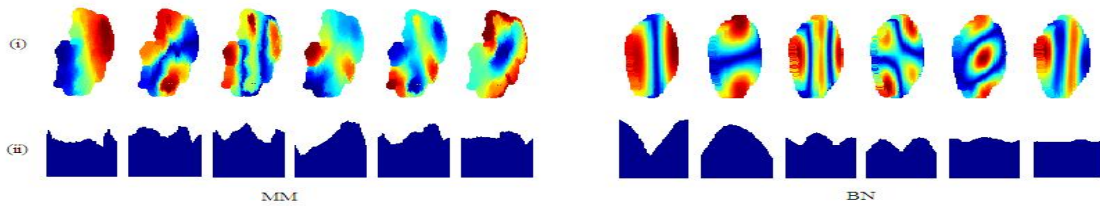


Figure 2: Visualization of the asymmetry descriptor of the MM and the BN in Figure.1. (i) The first six GPSs with the optimal T. (ii) Translated histograms given minimum asymmetry measures.

3 Experimental Results

The asymmetry descriptors for melanoma diagnosis is validated on 311 dermoscopy images with resolution ranging from 448×336 to 1098×826 pixels [11, 12]. There are 88 MMs and 223 BNs. The asymmetry feature vector is 6-dimensional with the minimum asymmetry measures obtained from red, green and blue channels in an RGB image, and their asymmetry measures in the direction perpendicular to the optimal reflectional axis.

3.1 Comparison with Asymmetry Detector without GPSs

In order to demonstrate the efficiency of the proposed asymmetry descriptor, we compute the shape and colour asymmetry descriptor without GPSs and compare the classification results with that from the descriptors in GPSs. The asymmetry detectors without GPSs are defined similarly as the proposed one. Specifically, a lesion is first segmented into 180 segments. Then each segment is represented by the proportion of segment areas in the whole lesion $SDes_l$, or by colour histogram $CDes_l$. Finally the asymmetry measure without GPSs can be quantified by minimizing the histogram differences in $[0 \pi]$ as (6).

$$SDes_l = \frac{N_l}{N}, \quad CDes_l = \frac{1}{N_l} \sum_{n=1}^{100} f(\text{colour}_l^n) * v(\text{colour}_l^n) \quad (5)$$

$$SAsy = \min(\sum_{l=1}^{90} \|SDes_l^I - SDes_l^R\|_2^2), \quad CAsy = \min(\sum_{l=1}^{90} \|CDes_l^I - CDes_l^R\|_2^2) \quad (6)$$

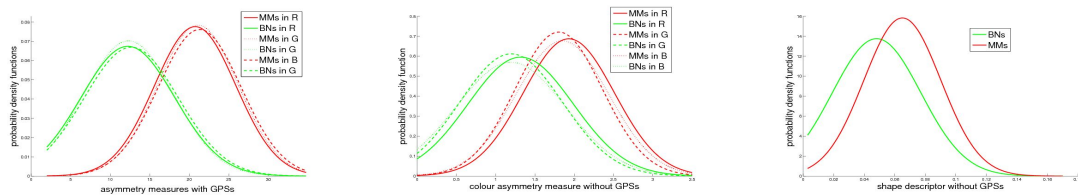


Figure 3: pdfs of the asymmetry descriptors. (a) the proposed asymmetry descriptor in GPSs. (b) colour asymmetry descriptor without GPSs. (c) shape asymmetry descriptor without GPSs.

Figure.3 plots the probability density functions (pdfs) of MMs and BNs calculated from the GPS-based descriptors, and the shape and colour asymmetry detectors without GPSs.

Compared the pdfs from measures without GPSs, the pdf computed in GPS spaces provides better distribution separation.

3.2 Performance Evaluation

Three different classifiers are applied to validate the classification accuracy, including Support Vector Machine (SVM), Artificial Neural Networks (ANN) and Bayesian classifier (BC). During the training-testing process, 155 dermatoscopy images are randomly selected for training and the other half of data are used for testing. For each classification algorithm, we automatically execute the program 30 times and record the average sensitivity, specificity and accuracy as the final classification results to complement the bias introduced by the insistence of random selection of the training data.

Table.1 shows the classification results of asymmetry descriptors with and without GPSs computed by 3 classifiers. Similar to the results in ure.3, the accuracy of the GPSs-based descriptor is approximately 4% higher than that of the combination of shape and colour descriptors without GPSs. The best diagnosis of the proposed asymmetry descriptor for testing data is 85.12% sensitivity and 76.38% specificity with the SVM classifier.

Table 1: Statistics of the classification results from asymmetry descriptors with and without GPSs.

	Training(%) (without/ with GPSs)			Testing(%) (without/ with GPSs)		
	Sensitivity	Specificity	Accuracy	Sensitivity	Specificity	Accuracy
SVM	86.65/ 88.17	77.15/ 81.50	79.84/ 83.39	82.94/ 85.12	70.96/ 76.38	74.08/ 78.85
ANN	76.08/ 79.80	74.89/ 75.42	75.23/ 76.66	75.10/ 76.33	69.70/ 74.28	71.24/ 74.86
BC	80.21/ 87.39	72.72/ 77.82	74.70/ 80.53	76.93/ 81.72	67.51/ 72.08	70.18/ 75.31

4 Conclusions

This paper proposes a novel histogram based reflectional asymmetry descriptor computed from global point signatures of the pigmentation model of the skin lesions. Experiments show that the proposed asymmetry descriptor is more efficient in distinguishing melanoma from benign nevi than the asymmetry detectors without GPSs. The classification results achieved by the SVM classifier proved competitive with 85.12% sensitivity and 76.38% specificity respectively.

References

- [1] A.Jerant,J.Johnson,C.Sheridan,T.Caffrey, Early Detection and Treatment of Skin Cancer, *Am.Fam.Physician*,vol.6,pp.357-368,2000.
- [2] W.Stoecker,W.Li,R.Moss, Automatic Detection of Asymmetry in Skin Tumors, *Computerized Medical Imaging and Graphics*,vol.16,pp.191-197,1992.
- [3] L.Andreassi,R.Perotti,P.Rubegni, Digital dermoscopy analysis for the differentiation of atypical nevi and early melanoma, *Arch Dermatol*,vol.135,pp. 1459-1465,1999.
- [4] M.dŠAmico,M.Ferri,I.Stanganelli, Qualitative Asymmetry Measure for Melanoma Detection,*IEEE International Symposium on Biomedical Imaging: Nano to Macro*,pp.1155-1158,2004.
- [5] T.Lee,V.Ng,R.Gallagher,A.Coldman,D.McLean, DullRazor: a software approach to hair removal from images, *Computers in Biology and Medicine*,vol.27,pp.533-543,1997.
- [6] C.Tomasi,R.Manduchi, Bilateral Filtering for Gray and Color Images, *In Proc. of IEEE International Conference on Computer Vision*,pp.839-846,1998.
- [7] Z.Liu,J.Sun,M.Smith,L.Smith,R.Warr, An automatic mean-shift based segmentation for pigmented skin lesions, *Medical Imaging Understanding and Analysis*,pp. 121-126,2010.
- [8] R.Rustamov, Laplace-beltrami Eigenfunctions for Deformation Invariant Shape Representation, *In Proc. of Symposium on Geometry Processing*,pp.225-233,2007.
- [9] M.Belkin,P.Niyogi,T.G.Dietterich,S.Becker,Z.Ghahramani, Laplacian eigenmaps and spectral techniques for embedding and clustering, *Advances in Neural Information Processing Systems*,vol.14,2002.MIT Press.
- [10] M.Ovsjanikov,J.Sun,L.Guibas, Global Intrinsic Symmetries of Shapes, *In Proc. of Eurographics Symposium on Geometry Processing*,vol.27,pp.1341-1348,2008.
- [11] E.Ehram, <http://dermoscopic.blogspot.com/>.
- [12] Dermatology Information System, <http://www.dermis.net/>.